Research Square

Preprints are preliminary reports that have not undergone peer review.
They should not be considered conclusive, used to inform clinical practice,
or referenced by the media as validated information.

De Novo Biosynthesis of Glycosylated Carotenoids in Escherichia Coli

Xixian Chen
Singapore Institute of Food and Biotechnology Innovation (SIFBI)
Xiaohui Lim
Singapore Institute of Food and Biotechnology Innovation (SIFBI)
Aurelie Bouin
Singapore Institute of Food and Biotechnology Innovation (SIFBI); TBI, Université de Toulouse
Thomas Lautier
Singapore Institute of Food and Biotechnology Innovation (SIFBI); TBI, Université de Toulouse
Congqiang Zhang (zcqsimon@outlook.com)
Singapore Institute of Food and Biotechnology Innovation (SIFBI) https://orcid.org/0000-0003-1070-8806

Research

Keywords: Carotenoids, metabolic engineering, synthetic biology, glycosylation, glucosyltransferase, zeaxanthin, astaxanthin, UPD-glucose.

Posted Date: May 6th, 2021

DOI: https://doi.org/10.21203/rs.3.rs-480662/v1

License: This work is licensed under a Creative Commons Attribution 4.0 International License.
Read Full License

Version of Record: A version of this preprint was published at Bioresources and Bioprocessing on July 29th, 2021. See the published version at https://doi.org/10.1186/s40643-021-00415-0.

De novo biosynthesis of glycosylated carotenoids in *Escherichia coli*

Xixian Chen[1], Xiao Hui Lim[1], Aurelie Bouin[1,2], Thomas Lautier[1,2], Congqiang Zhang[1*]

*[1]Singapore Institute of Food and Biotechnology Innovation (SIFBI), Agency for Science, Technology and Research (A*STAR), Singapore.*

[2]TBI, Université de Toulouse, CNRS, INRAE, INSA, Toulouse, France

* To whom correspondence should be addressed.

Congqiang Zhang**:** SIFBI, A*STAR, Proteos level 4, Singapore 138673;

Email: zcqsimon@outlook.com; congqiang_zhang@sifbi.a-star.edu.sg

Abstract

Carotenoids have wide applications in food, feed, pharmaceutical and cosmetic industries. The fast-growing market demands highlight the importance of developing new routes for carotenoid biosynthesis. Meanwhile, a complementary need is to improve low bioavailability because of the hydrophobicity of carotenoids. One solution is glycosylation,

which can substantially increase the water solubility of carotenoids, and enhance the bioavailability, photostability and biological activities as food supplements and medicines. Here, we report metabolic engineering efforts to produce glycosylated carotenoids in *Escherichia coli*. By fine tuning the 14 gene pathway, our strain produced up to 47.2 mg/L (~11670 ppm) of zeaxanthin glucosides, ~78% of the total carotenoids produced. In another construct with 15-gene pathway, the strain produced a mixture of carotenoid glucosides including astaxanthin and adonixanthin glucosides with a total yield of 8.1 mg/L (1774 ppm). Our work demonstrated a proof-of-concept study for the microbial biosynthesis of glycosylated carotenoids. (145 words)

Keyword: Carotenoids, metabolic engineering, synthetic biology, glycosylation, glucosyltransferase, zeaxanthin, astaxanthin, UPD-glucose.

Introduction

Carotenoids (>1,100) are natural pigments widely distributed in plants, animals, algae and microbes (Yabuzaki 2017; Zhang 2018). The structures of carotenoids typically consist of an electron-rich polyene chain with nine or more conjugated double bonds. This unique feature contributes primarily to their photo-protection and light-harvesting property, antioxidant activities to quench free radicals and singlet oxygen, and vivid colors (Sandmann 2019). Carotenoids function as photosynthesis and photoprotection agents in photosynthetic organisms (e.g., plants and algae) and protect non-photosynthetic organisms (e.g., bacteria, archaea and fungi) from photooxidative damages (Hashimoto et al. 2016). Carotenoids also serve as structural molecules by integrating in lipid membranes, hence, modulating membrane fluidity (Richter et al. 2015). Because of these properties, especially for the pigment and health benefits, carotenoids have various applications in food, feed, nutraceutical and pharmaceutical industries, and the industrial demand is growing rapidly. For example, the global market of astaxanthin is projected to reach $2.57 billion worldwide by 2025 (Zhang et al. 2020).

However, most natural carotenoids are lipophilic and hardly soluble in water. The hydrophobicity of carotenoids limits their application in medicine and food where enhanced water dispensability is required to facilitate their effective uptake or use (Dembitsky 2005; Hada et al. 2012). Therefore, several attempts, mainly chemical approaches (e.g., converting carotenoids to salts of carotenoid esters, or forming carotenoid-cyclodextrin complex), have been made to increase the carotenoid hydrophilicity (Hada et al. 2012). Alternatively, glycosylation is an excellent natural way to increase carotenoid solubility. In nature, a large number of hydrophobic natural products (e.g., lipids and terpenes) are

glycosylated into more water-soluble products by glycosyltransferases (Elshahawi et al. 2015). In fact, water-soluble carotenoids, although rare, are present in nature, such as crocins (or glycosyl polyene esters) in saffron (Dembitsky 2005). In addition, several other glycosylated carotenoids are uncovered in various microbes, such as zeaxanthin glucoside (Misawa et al. 1990), astaxanthin glucoside (Yokoyama et al. 1998), adonixanthin-β-D-glucoside (Yokoyama et al. 1995), sioxanthin (Richter et al. 2015) and a C50 decaprenoxanthin diglucoside (Krubasik et al. 2001).

Natural metabolites are typically produced meaningfully with biological functions for host living organisms. Primary metabolites are synthesized to support their growth and development. Secondary metabolites typically increase the competitiveness of the organism within its environment. Likewise, glycosylated carotenoids should have meaningful functions for their hosts. It is reported that glycosylated carotenoids play important roles in maintaining cell wall structure and their localization stabilizes the thylakoid membrane in cyanobacteria where the glycosyl moiety serves as a binding motif that enables the proper folding and stacking of the thylakoid membrane (Mohamed et al. 2005). The first bacterial gene that encodes the enzyme to catalyze carotenoid glycosylation was identified in *Pantoea ananatis* (previously as *Erwinia uredovora*) (Misawa et al. 1990) and it was reported that glycosylation can alter carotenoid deposition in plants (Wurtzel 2019). As a phytopathogen, this might contribute to the virulence of *P. ananatis* with host plant cells. Moreover, carotenoid glucosides contribute to the heat resistance of the *Thermus* species, and hence, are also named thermoxanthins (Hada et al. 2012). As for commercial applications, apart from improved water solubility (e.g., the solubility of zeaxanthin, zeaxanthin mono- and diglucosides are 12.6, 100 and 800 ppm in water, respectively (Hundle et al. 1992)), glycosylation of carotenoids also leads to

structural diversity and several other benefits, such as increased bioavailability and efficacy as food supplements and medicines, and improved photostability (Polyakov et al. 2009) and biological activities (e.g., antioxidant activity) of carotenoids (Matsushita et al. 2000). It is proposed that the increase in antioxidant activities is not from their intrinsic ability of additional glucosides to scavenge free radicals, but arises from the enhanced affinity with singlet oxygen, the location and orientation in cells (Choi et al. 2013; Matsushita et al. 2000).

Carotenoids are glycosylated by glycosyltransferases (GTs), which is a large enzyme family. GTs typically catalyze a hydroxyl or carboxyl group of lipophilic substrates as the substituent moiety for glycosylation. For carotenoid glycosylation, the hydroxyl group is the commonest substituent moiety, and the carotenoid GTs belong to GT family 1 or GT1. Uridine diphosphate-α-D-glucose (UDP-glucose) is the most abundant sugar donor to carotenoid glycosylation. In addition, other sugars such as L-rhamnose, L-fucose, D-xylose and L-quinovose can also be recruited especially in cyanobacteria (Choi et al. 2013).

To date, only a couple of studies have demonstrated the biosynthesis of carotenoid glucosides in *Escherichia coli* and in several natural microbial producers (Choi et al. 2013; Misawa et al. 1990; Yokoyama et al. 1995; Yokoyama et al. 1998). However, these studies only produced detectable amount of carotenoid glucosides and were far from the minimal requirement for industrial applications. Here, using the zeaxanthin glucosyltransferase (ZGT, the gene *crtX*, UniProt ID D4GFK6) from *P. ananatis*, we have constructed a 14- and 15-gene pathway in *E. coli* to synthesize various carotenoid glucosides, such as zeaxanthin D-glucoside (yellow) and astaxanthin D-glucoside (red). The carotenoid yields

have been improved by rational metabolic engineering approaches and bioprocess optimization.

Results

The pathway design for glycosylated carotenoids

The metabolic pathway for glycosylated carotenoids was designed on top of our previous optimized astaxanthin strain (Zhang et al. 2018). Briefly, the mevalonate pathway genes were cloned into the modules 1 (AHT, the genes *atoB*, *hmgB* and truncated *hmgR*) and 2 (MPPI, the genes *mevk*, *pmk*, *pmd* and *idi*) and the lycopene pathway genes (*crtEBI* and *ispA*) were located in module 3 (EBIA). The last module (module 4, YZX or YZWX) consists of the genes to produce zeaxanthin glucosides (*crtY, crtZ*, *and crtX*) or to produce astaxanthin glucosides (*crtY, crtZ, crtW*, and *crtX*) (Figure 1). All the modules were controlled by T7 and its variants (e.g., TM1, TM2 and TM3) and induced by isopropyl β-d-1-thiogalactopyranoside (IPTG) (Zhang et al. 2015). This modular arrangement provides the flexibility to balance the global pathways (14-15 genes) and to fine tune the local pathways (e.g., module 4). In addition, as the module 4 controls the cyclization (*crtY*), hydroxylation (*crtZ*), ketolation (*crtW*), and glycosylation (*crtX*) of carotenoids, it is relatively simple to switch from one carotenoid (e.g., using *crtYZ* to produce zeaxanthin) to another one (e.g., using *crtYZWX* to astaxanthin glucoside) without modifying the upstream pathways genes.

The production of glycosylated zeaxanthin

Firstly, we used the modules 1-3 and the module 4 (YZX) to demonstrate the capability to produce zeaxanthin glucoside. We developed a LC-TOF-MS method to detect the carotenoids and their glucosides (summary in Table 1). In the constructed strain with *crtX*, we managed to detect five carotenoids: lycopene, β-carotene, zeaxanthin, zeaxanthin-β-D-glucoside and zeaxanthin-β-D-diglucoside, whereas the control strain without *crtX* did not produce either glycosylated zeaxanthin (Figure 2A). The intermediate β-cryptoxanthin was not detected in either strain. The LC chromatograms and mass spectra for zeaxanthin (m/z 568.428, Table 1), zeaxanthin-β-D-glucoside (m/z 730.481) and zeaxanthin-β-D-diglucoside (m/z 892.534) were shown in Figures 2A and B. In addition, we also purified some zeaxanthin glucosides from the strain with *crtX* and obtained a yellow aqueous solution (~30 mg/L). In contrast, zeaxanthin barely dissolves in water leading to a transparent water solution (Figure 2C).

Optimization of glycosylation of zeaxanthin

In our first design strain X0, the glycosylation of zeaxanthin was incomplete: ~26.8 % of monoglycosylated and 59.0% of diglycosylated (here the percentage was calculated by normalizing to the total yield of zeaxanthin and its two glucosides) and 14.2% of zeaxanthin remained unglycosylated (Figure 3A and B). We hypothesized that glycosylation of zeaxanthin could be limited by insufficient activity of ZGT. To test it, we re-designed another four ribosomal binding sites (RBSs) of *crtX* which have relatively higher translational efficiencies than the initial RBS in strain X0 (Figure 3C). Indeed, we observed that using stronger RBS for ZGT (*crtX*) led to higher glycosylation of zeaxanthin (Figure 3A and D). Strain X1 had the strongest RBS and produced the highest amount of

143 zeaxanthin-β-D-diglucoside (~3139 ppm and ~87.4% of total zeaxanthin and its
144 glucosides). We attempted to correlate RBS strengths to zeaxanthin-β-D-diglucoside
145 production. Zeaxanthin-β-D-glucoside produced appears to reach a saturated percentage
146 when RBS relative strength was higher than 0.3 (Figure 3D).

147 Next, we evaluated the effect of different carbon sources on the biosynthesis of zeaxanthin
148 glucosides. As an abundant and inexpensive carbon source, we chose glucose and
149 hypothesized that glucose might be advantageous to supply additional UDP-glucose,
150 which is the key cofactor for carotenoid glycosylation. UDP-glucose can be produced from
151 glucose with three enzymes: *glk*: glucokinase, *pgm*: phosphoglucomutase, galU: UDP-
152 glucose pyrophosphorylase (Mao et al. 2006; Shrestha et al. 2019). In addition, we also
153 chose glycerol as it is inexpensive and was reported to favour carotenoid production
154 (Zhang et al. 2013). For X1 strain, the glucose supplementation (10 g/L) led to higher
155 production of zeaxanthin glucosides (~3650 ppm) than the supplementation of 10 g/L of
156 glycerol or the mixture of glucose (5 g/L) and glycerol (5 g/L) (Figure 4A). Subsequently,
157 we increased the amount of supplemented glucose from 10 to 20 g/L, the yield of
158 zeaxanthin diglucoside was further increased from ~3400 (or 15.1 mg/L) to ~4690 ppm (or
159 25.3 mg/L). At the same time, OD_{600} was also increased from 10.8 to 13.1 (Figure 4B). Of
160 the total carotenoids produced including lycopene and β-carotene, zeaxanthin glucosides
161 reached about 64% in X1 strain.

162 In addition, we also observed that lycopene was accumulated as the main intermediate
163 carotenoid for all the strains and conditions in Figures 3A and 4A. We hypothesized that
164 the accumulation of lycopene could arise from the insufficient activity of lycopene cyclase
165 (or *crtY*, Figure 1). Indeed, the introduction of extra copies of *crtY* ("+crtY" strain)

significantly boosted zeaxanthin diglucoside yield from 3400 to 7150 ppm (or 23.1 mg/L) and zeaxanthin glucoside yield from 350 to 4520 ppm (14.6 mg/L) in the medium supplemented with 10 g/L glucose (Figure 4B). Furthermore, for the "+crtY" strain, the titres of zeaxanthin diglucoside and glucoside were further increased to 31.0 and 16.3 mg/L, respectively, as the supplemented glucose was increased from 10 to 20 g/L (Figure 4B). Lastly, the yields of zeaxanthin glucosides of "+crtY" strain were about 78% of that of total carotenoids produced.

Distribution of carotenoids in *E. coli* cells

While studying the zeaxanthin glucoside strain, we observed that some cells of zeaxanthin production strain were longer than others in microscopes (Figure 5A). In comparison, there were no elongated cells for zeaxanthin glucoside production strain. We wondered if the cell shape difference was attributed to the higher hydrophilicity of zeaxanthin glucosides so that most zeaxanthin glucosides may be distributed in cytosol. To test the hypothesis, we analysed the distribution of carotenoids between cytosol and membrane. Unexpectedly, it was found that all the four carotenoids (lycopene, β-carotene, zeaxanthin and zeaxanthin glucosides) were predominantly localized in membrane (Figure 5B). Less than 2% of them were present in cytosol. In addition, less zeaxanthin glucosides (0.08%) was distributed in cytosol as compared to zeaxanthin (1.13%). Our data supported the notion that zeaxanthin and its glucosides might have higher affinity with membrane than cytosol. Structurally, the glucoside and carotene of carotenoid glucosides resemble the hydrophilic head and the hydrophobic tail of phospholipid bilayers, respectively; also, the dimension of bilayer inner membrane (37.5 ±0.5 Å) (Mitra et al. 2004) is close to that of zeaxanthin diglucoside (~30Å) (Figure 5B). Carotenoid glucosides are reported to be

clustered in rigid patches and such local rigidity can protect the membrane integrity under internal or external stress (e.g., oxidative and extreme temperature) (Mohamed et al. 2005). This might attribute to cell shape difference between zeaxanthin and zeaxanthin-glucoside producing cells, and further study is warranted to explore the mechanism.

The production of glycosylated astaxanthin

After demonstrating our design was working for zeaxanthin glycosylation, we further tested the other design with module YZWX to produce astaxanthin glucosides. With the addition of the gene *crtX* in one of our best astaxanthin producer strains (Ast strain, Figure 6A and B) (Zhang et al. 2018), we tested the astaxanthin glycosylation capability (the resulting strain was named GA01). Overall, seven carotenoid glucosides are detected in GA01: zeaxanthin-β-D-glucoside, adonirubin-β-D-glucoside (m/z 742.444), adonixanthin-β-D-glucoside (m/z 744.460), astaxanthin-β-D-glucoside (m/z 758.439), zeaxanthin-β-D-diglucoside, adonixanthin-β-D-diglucoside (m/z 906.513) and astaxanthin-β-D-diglucoside (m/z 920.492, Figure 6A and B, Table 1, mass spectra in Figures 6C and Supplementary Figure S1, and LC chromatograms in Supplementary Figure S2 and S3). Among them, astaxanthin-β-D-glucoside was the main glycosylated product with a yield of 4.51 mg/L (968 ppm), about 68% of total carotenoid glucosides. In addition, about 4.82 mg/L astaxanthin (1035 ppm) was not glycosylated and larger amount of β-carotene (16.0 mg/L, 3426 ppm) remained in GA01 strain. Furthermore, we observed that the introduction of *crtX* resulted in the total carotenoid yields in GA01 strain dropped by 54%, as compared to its parental Ast strain (Figure 6A), which might be due to the overall perturbation to the mevalonate and carotenoid pathway carbon fluxes or feedback regulations.

Optimization of glycosylation of astaxanthin

Moreover, the higher IPTG concentration reduced the total yield of glycosylated carotenoids from 6.61 to 3.60 mg/L (1418 to 799 ppm) and non-glycosylated (or aglycones) carotenoids from 24.8 to 15.7 mg/L (5320 to 3485 ppm, Figure 6A), possibly because IPTG perturbed the whole biosynthetic pathway where all the genes were controlled by T7 promoter variants and/or it promoted a competition between CrtZ and CrtW with intermediate accumulation (Figure 1). It has been observed that the translational efficiency of the β-carotene hydroxylase (*crtZ*) is more crucial than that of β-carotene ketolase (*crtW*) on astaxanthin production (Zhang et al. 2018). Therefore, we used nine different ribosomal binding sites (RBSs, Supplementary Table S1) covering from 1% to 100% of translational efficiencies (the strains were named G01-09, translational efficiencies were normalized to that of strain GA01, the strongest among them) to optimize the production of glycosylated carotenoids, especially glycosylated astaxanthin.

Essentially, GA01-09 were strains with the same design except for the different RBSs of *crtZ* (Supplementary Table S1). Indeed, the RBS had marked effects on the carotenoid production and distribution (Figure 6A and B, Supplementary Figure S4). For GA08 and GA09, the total carotenoid yields were very low, below 10 mg/L (<2000 ppm), and the carotenoid glucosides were also very low, below 0.4 mg/L (<100 ppm). GA01 and GA02 had the highest glycosylation efficiency (~21%, Figure 6A), but with relatively lower total carotenoid yields as compared to GA03, GA04 and GA05. Surprisingly, GA03, with a relatively weaker RBS (Supplementary Table S1), had the highest yield of total carotenoids (11623 ppm) and total glycosylated carotenoids (1774 ppm). Similar to GA01, strains GA02-07 had lower yields of carotenoids (including glycosylated carotenoids)

when IPTG concentrations increased from 0.03 to 0.1 mM. In contrast, strains GA08-09 had higher yields when IPTG dosage increased, likely due to the relatively weaker RBSs of *crtZ*.

RBS engineering of *crtZ* has enhanced the production of glycosylated and total carotenoids by 25% and 72%, respectively, as compared to that of GA01. However, unlike the obvious positive effect of RBS of *crtX* on zeaxanthin glucosides (Figure 3D), the data in Supplementary Figure S4 indicated the lack of correlation between the RBS strength of *crtZ* and carotenoid production. The lack of correlation was not surprising as the top two producers, GA03 and GA05, had relative weaker RBSs.

Discussion

Here, we successfully engineered *E. coli* to produce carotenoid glucosides in high amounts. Particularly, our zeaxanthin-glucoside strain produced 11670 ppm of two zeaxanthin glucosides (~7150 ppm of zeaxanthin diglucose, ~4520 ppm of zeaxanthin glucoside) in 2-day batch fermentation (Figure 4B). In contrast, the astaxanthin-glucoside strains (GA01-09) produced lower amount of total carotenoid glucosides (1774 ppm) but with high diversity where 7 carotenoid glucosides were detected. To the best of our knowledge, our study is the first to produce these carotenoid glucosides (up to 7 varieties) in recombinant microbes.

Our results here supported that ZGT, belonging to the GT1 family, was able to glycosylate various other carotenoids (e.g., adonirubin, adonixanthin), in addition to the reported zeaxanthin and astaxanthin (Hundle et al. 1992; Yokoyama et al. 1998). Furthermore, if

256 xanthophylls have two hydroxyl groups (e.g., astaxanthin), di-glycosylated products can
257 also be produced by ZGT. Considering the complexity of the carotenoid pathway and the
258 promiscuity of ZGT, the product diversity was not surprising as the glycosylation reaction
259 competed with other reactions (hydroxylation or ketolation, Figure 1). The presence of
260 bulky glycoside moiety may prevent the glycosylated intermediates (e.g., zeaxanthin and
261 adonixanthin) from further ketolation to astaxanthin glucosides by the β-carotene ketolase
262 (*crtW*), hence, all the carotenoid glucosides became the end products (Figure 1).

263 To improve the glycosylation of zeaxanthin, we have employed RBS engineering (strong
264 RBS for ZGT), media optimization and supplementation of additional lycopene cyclase
265 (*crtY*). All the strategies were very effective, collectively, they enhanced the yields of the
266 two zeaxanthin glucosides from 1640 ppm to 11670 ppm, or by 7.1 fold. However, it was
267 not straightforward for astaxanthin glycosylation. A possible reason is that the ZGT from
268 *P. ananatis* might have relatively lower activity for astaxanthin than zeaxanthin. The keto
269 group may also stabilize the hydroxyl group or introduces steric hinderance and thus
270 reduces accessibility by ZGT. Also, the competitions for carotenoid intermediates by
271 ketolases (CrtW), hydroxylases (CrtZ) and ZGT increase the ramification of the metabolic
272 pathway. To further improve the production of astaxanthin glucosides, four strategies can
273 be employed in the future: (1) to explore the natural diversity of ZGTs for more suitable
274 enzymes; (2) to balance the expression of Module 4 (Figure 1); (3) to further manipulate
275 the intracellular UDP-glucose supply; 4) to implement a dynamic regulation to trigger
276 glycosylation after the formation of astaxanthin. A search in UniProt database resulted in
277 254 zeaxanthin GT homologues from 69 microbial genera, particularly in *Pseudomonas*,
278 *Pantoea* and *Massilia*, which have 88, 22, 12 of homologues identified, respectively.
279 Experimental screening may lead to identifying some candidates with higher activities

and/or specificities for astaxanthin. Furthermore, the data in Figures 3 and 6 indicated that the perturbation of *crtZ* and *crtX* expression had strong effects on both yields of total carotenoids and glycosylated carotenoids. The parental strain (Ast) had produced astaxanthin as the main product, however, all the GA01-09 strains had β-carotene accumulated intracellularly (Figure 6B). This indicated that previously balanced pathway was perturbed by the introduction of ZGT. A solution is to refine the module 4 by RBS/promoter engineering or organisation shuffling of operon genes to minimizing the accumulation of intermediates (e.g., lycopene and β-carotene, Figure 6B). Lastly, unlike zeaxanthin glycosylation strain with high glycosylation efficiency (>90%), the astaxanthin glycosylation was relatively low (40-50%) indicating they might be still limited by the accessible intracellular UDP-glucose, whose supply can be enhanced by overexpressing UDP-glucose biosynthetic pathway genes (e.g., *glk*: glucokinase, *pgm*: phosphoglucomutase, *galU*: UDP-glucose pyrophosphorylase) and by utilizing other types of UDP-sugars with glycosyltransferases. The strategy has been successfully applied to increase the production of flavonoids such as anthocyanins (Shrestha et al. 2019; Zha et al. 2020) and is worth exploring on carotenoid glycosylation.

Conclusion

We have developed microbial strains to overproduce various carotenoid glucosides. The metabolic engineering and bioprocess strategies are proven to be effective and have synergic effects in improving the yields of carotenoid glucosides by balancing the metabolic pathways and supplying carbon precursors and important cofactors. Our study here demonstrated a proof-of-concept study for microbial production of glycosylated

carotenoids and might inspire the production for other high-value metabolites, especially other glycosylated metabolites.

Methods

Strain and plasmid construction

E. coli Bl21-Gold DE3 strain (Stratagene) was used in this study. The plasmids p15A-*spec-hmgS-atoB-hmgR* (L2-8), p15A-*spec-crtY-hmgS-atoB-hmgR* (L2-8) p15A-*cam-mevK-pmk-pmd-idi* (L2-5), p15A-*kan-crtEBI-ispA* were designed as previously described (Zhang et al. 2018). The zeaxanthin GT gene *(crtX)* from *Pantoea ananatis* was inserted in the operon of the plasmids p15A-amp-crtYZ (L2-9) and p15A-amp-crtYZW (L2-9) (Zhang et al. 2018) to obtain p15A-amp-crtYZX and p15A-amp-crtYZWX, respectively.

Construction of RBS library

CrtZ RBS library was created using the degenerate primer and followed by screening and sequencing validations, using the same cloning method as previously described (Zhang et al. 2018). RBS strengths or translation efficiencies were predicted by RBS Calculator, version 2.0 (Farasat et al. 2014).

Tube culture of the *E. coli* strains

The medium used was TB medium (20 g/L tryptone, 24 g/L yeast extract, 17 mM KH_2PO_4, and 72 mM K_2HPO_4) and 2XPY medium (20 g/L peptone, 10 g/L yeast extract and 10 g/L NaCl), supplemented with 10 g/L glycerol or 10-20 g/L glucose or their mixture (5 g/L glucose + 5 g/L glycerol), 50 mM 4-(2-hydroxyethyl)-1-piperazineethanesulfonic acid

(HEPES), as previously described (Zhang et al. 2018). For strain optimization, the cells were grown in 1 mL of TB or 2XPY medium in 14 ml BD Falcon™ tube at 28 °C/250 rpm for 2-3 days. The cells were also grown in 50 mL culture in shaking flasks for validation of the carotenoid production. The cells were initially grown at 37 °C/250 rpm until OD_{600} reached ~0.8, induced by 0.03-0.1 mM IPTG, and were subsequently grown at 28 °C for 2 days. The antibiotics (34 μg/ml chloramphenicol, 50 μg/ml kanamycin, 50 μg/ml spectinomycin and 100 μg/ml ampicillin) were supplemented in the culture to maintain the four plasmids.

Microscope imaging of *E. coli* cells

For microscopy assay, *E. coli* cells were directly sampled from cell cultures. Cell amount was normalized by OD_{600} and directly observed at 1000 magnitude using a Leica DM6000B microscope. Neither centrifuge nor washing steps was introduced to avoid perturbation of the cell morphologies.

Extraction and quantification of carotenoids

Total intracellular carotenoids were extracted from cellular pellets according to the acetone extraction method (Zhang et al. 2018). Briefly, 10–50 μL bacterial culture (depending on the content of carotenoids in the cells) was collected and centrifuged. Cell pellets were washed with PBS and were resuspended in 20 μL of water, followed by addition of 180 μL of acetone and and vigorous homogenization for 20 min. After 10 minutes of centrifugation at 14,000 *g*, the supernatant was collected and filtered using a PTFE, 0.45μm filter.

The separation of carotenoids from cytosol and cell membranes was done by differential centrifugation. Briefly, cell pellets collected from 1mL of culture were resuspended in 1ml

lysis buffer (50mM Tris HCl of pH 7.5, 200mM NaCl, 1 mg/ml lysozyme of pH 8) before 3x30 sec sonication at 4 °C (75% amplitude). The cell lysate was subsequently centrifugated for 10 minutes at 14,000 *g*. The supernatant containing the cytosol fraction of carotenoids and the pellet debris containing the membrane fraction were extracted separately with by 1mL of extraction buffer (hexane: acetone: ethanol at 2:1:1 volumetric ratio).

Quantification of carotenoids

All the carotenoids were analysed by Agilent 1290 Infinity II UHPLC System coupled with Diode Array Detector (DAD) detector and 6230B TOF MS platform. The LC/MS method was similar to previously described (Zhang et al. 2018). Briefly, 1 μL of purified carotenoids in acetone was injected into the Agilent ZORBAX RRHD Eclipse Plus C18 2.1X50 mm, 1.8 um. Separation was carried out at a flow rate of 0.5 mL/min. The mobile phase and gradient used were as follows. The analysis started from 10% water (0.1% formic acid), 10% methanol (0.1% formic acid) and 80% acetonitrile (0.1% formic acid) and this condition was maintained for 2 min, followed by the increase in methanol from 10% to 90% and the decrease in water from 10% to 0 and acetonitrile from 80% to 10% within 0.1 min. The condition (90% methanol and 10% acetonitrile) was continued for 7 min. The whole analysis finished at 10 min. Mass spectrometry was operated to scan 100-1100 m/z in ESI-positive mode with 4000 V capillary voltage. Nebulizer gas was supplied at 35 psig and dry gas flow was 10 L/min. Gas temperature was set at 325 °C. Shealth gas was set at 350 °C and 12 L/min. Retention time was determined with chemical standards or calculated based on chromatography profile for those carotenoids without standards.

Carotenoid concentrations were calculated based on the peak area of each compound extracted by their corresponding m/z value (Table 1) or UV absorbance at 450 nm (Supplementary Figure S2). Standard curves were generated for the five chemical standards with extracted-ion chromatogram (EIC) peak areas (Supplementary Figure S3): lycopene, β-carotene, astaxanthin, canthaxanthin (Sigma-Aldrich, St. Luis, MO, USA), and zeaxanthin (Santa Cruz Biotechnology, Dallas, TX, USA). For those carotenoids without standards, the concentration was calculated based on the relative peak area to its close compartment. For example, the concentrations of zeaxanthin glucoside and zeaxanthin diglucoside were calculated based on that of zeaxanthin; the concentrations of astaxanthin glucosides, adonixanthin and its diglucosides were calculated based on that of astaxanthin. Carotenoid contents were calculated by normalizing the titres with dry cell weight (μg carotenoids per gram DCW, or ppm) (Zhang et al. 2018).

Data availability

All data supporting the findings of this study are available in the article, Supplementary Information, or upon request from the corresponding author.

Abbreviations

GT: glycosyltransferase; UDP-glucose: Uridine diphosphate-α-D-glucose; ZGT, zeaxanthin glucosyltransferase; IPTG, isopropyl β-d-1-thiogalactopyranoside; RBS: ribosomal binding site.

Declarations

Ethics approval and consent to participate

Not applicable.

Consent for publication

The publication of the paper has been agreed by the authors.

Competing interests

The authors declare that they have no potential conflicts of interest.

Funding

This research was supported by AME Young Individual Research Grant (YIRG) A2084c0064 (Dr Congqiang Zhang) and A1984c0040 (Dr Xixian Chen), Agency for Science, Technology and Research (A*STAR), Singapore.

Acknowledgements

We acknowledge Prof Heng-Phon Too, National University of Singapore, Dr Nicholas David Lindley, Dr Ee Lui Ang and Dr Hazel Khoo, Singapore Institute of Food and Biotechnology Innovation, for the support and insightful suggestions of the project.

Author contributions

C.Z. conceived the project, analyzed the results, and wrote the manuscript. X.C., X.L., and C.Z designed and did the experiments of strain engineering. T.L. and A.B. designed and did the microscope imaging of *E. coli* and quantification of carotenoid distributed in

membrane and cytosol. All authors contributed to the discussion and approved the final manuscript.

Reference

Choi SK, Osawa A, Maoka T, et al. (2013) 3-beta-Glucosyl-3'-beta-quinovosyl zeaxanthin, a novel carotenoid glycoside synthesized by Escherichia coli cells expressing the Pantoea ananatis carotenoid biosynthesis gene cluster. Appl Microbiol Biotechnol 97(19):8479-86. doi:10.1007/s00253-013-5101-9

Dembitsky VM (2005) Astonishing diversity of natural surfactants: 3. Carotenoid glycosides and isoprenoid glycolipids. Lipids 40(6):535-57. doi:10.1007/s11745-005-1415-z

Elshahawi SI, Shaaban KA, Kharel MK, Thorson JS (2015) A comprehensive review of glycosylated bacterial natural products. Chem Soc Rev 44(21):7591-697. doi:10.1039/c4cs00426d

Farasat I, Kushwaha M, Collens J, et al. (2014) Efficient search, mapping, and optimization of multi-protein genetic systems in diverse bacteria. Mol Syst Biol 10(6):731-731. doi:10.15252/msb.20134955

Hada M, Nagy V, Deli J, Agocs A (2012) Hydrophilic carotenoids: recent progress. Molecules 17(5):5003-12. doi:10.3390/molecules17055003

425 Hashimoto H, Uragami C, Cogdell RJ (2016) Carotenoids and Photosynthesis. In: Stange
426 C (ed) Carotenoids in Nature: Biosynthesis, Regulation and Function. Springer
427 International Publishing, Cham, pp 111-139

428 Hundle BS, O'Brien DA, Alberti M, et al. (1992) Functional expression of zeaxanthin
429 glucosyltransferase from Erwinia herbicola and a proposed uridine diphosphate binding
430 site. Proc Natl Acad Sci U S A 89(19):9321-5. doi:10.1073/pnas.89.19.9321

431 Krubasik P, Takaichi S, Maoka T, et al. (2001) Detailed biosynthetic pathway to
432 decaprenoxanthin diglucoside in Corynebacterium glutamicum and identification of novel
433 intermediates. Arch Microbiol 176(3):217-223. doi:10.1007/s002030100315

434 Mao Z, Shin HD, Chen RR (2006) Engineering the E. coli UDP-glucose synthesis pathway
435 for oligosaccharide synthesis. Biotechnol Prog 22(2):369-74. doi:10.1021/bp0503181

436 Matsushita Y, Suzuki R, Nara E, et al. (2000) Antioxidant activity of polar carotenoids
437 including astaxanthin-β-glucoside from marine bacterium on PC liposomes. Fisheries
438 Science 66(5):980-985. doi:10.1046/j.1444-2906.2000.00155.x

439 Misawa N, Nakagawa M, Kobayashi K, et al. (1990) Elucidation of the Erwinia uredovora
440 carotenoid biosynthetic pathway by functional analysis of gene products expressed in
441 Escherichia coli. J Bacteriol 172(12):6704-12. doi:10.1128/jb.172.12.6704-6712.1990

442 Mitra K, Ubarretxena-Belandia I, Taguchi T, et al. (2004) Modulation of the bilayer
443 thickness of exocytic pathway membranes by membrane proteins rather than cholesterol.
444 Proc Natl Acad Sci U S A 101(12):4083-8. doi:10.1073/pnas.0307332101

445 Mohamed HE, van de Meene AM, Roberson RW, Vermaas WF (2005) Myxoxanthophyll
446 is required for normal cell wall structure and thylakoid organization in the cyanobacterium
447 Synechocystis sp. strain PCC 6803. J Bacteriol 187(20):6883-92.
448 doi:10.1128/JB.187.20.6883-6892.2005

449 Polyakov NE, Leshina TV, Meteleva ES, et al. (2009) Water Soluble Complexes of
450 Carotenoids with Arabinogalactan. The Journal of Physical Chemistry B 113(1):275-282.
451 doi:10.1021/jp805531q

452 Richter TK, Hughes CC, Moore BS (2015) Sioxanthin, a novel glycosylated carotenoid,
453 reveals an unusual subclustered biosynthetic pathway. Environ Microbiol 17(6):2158-71.
454 doi:10.1111/1462-2920.12669

455 Sandmann G (2019) Antioxidant Protection from UV- and Light-Stress Related to
456 Carotenoid Structures. Antioxidants (Basel) 8(7):219. doi:10.3390/antiox8070219

457 Shrestha B, Pandey RP, Darsandhari S, et al. (2019) Combinatorial approach for
458 improved cyanidin 3-O-glucoside production in Escherichia coli. Microb Cell Fact 18(1):7.
459 doi:10.1186/s12934-019-1056-6

460 Wurtzel ET (2019) Changing Form and Function through Carotenoids and Synthetic
461 Biology. Plant Physiol 179(3):830-843. doi:10.1104/pp.18.01122

462 Yabuzaki J (2017) Carotenoids Database: structures, chemical fingerprints and
463 distribution among organisms. Database: The Journal of Biological Databases and
464 Curation 2017:bax004. doi:10.1093/database/bax004

Yokoyama A, Adachi K, Shizuri Y (1995) New Carotenoid Glucosides, Astaxanthin Glucoside and Adonixanthin Glucoside, Isolated from the Astaxanthin-Producing Marine Bacterium, Agrobacterium aurantiacum. J Nat Prod 58(12):1929-1933. doi:10.1021/np50126a022

Yokoyama A, Shizuri Y, Misawa N (1998) Production of new carotenoids, astaxanthin glucosides, by *Escherichia coli* transformants carrying carotenoid biosynthesis genes. Tetrahedron Lett 39(22):3709-3712. doi:10.1016/s0040-4039(98)00542-5

Zha J, Wu X, Koffas MA (2020) Making brilliant colors by microorganisms. Curr Opin Biotechnol 61:135-141. doi:10.1016/j.copbio.2019.12.020

Zhang C (2018) Biosynthesis of Carotenoids and Apocarotenoids by Microorganisms and Their Industrial Potential. Progress in Carotenoid Research:85.

Zhang C, Chen X, Too H-P (2020) Microbial astaxanthin biosynthesis: recent achievements, challenges, and commercialization outlook. Appl Microbiol Biotechnol 104(13):5725-5737. doi:10.1007/s00253-020-10648-2

Zhang C, Chen X, Zou R, et al. (2013) Combining genotype improvement and statistical media optimization for isoprenoid production in *E. coli*. PLoS ONE 8(10):e75164. doi:10.1371/journal.pone.0075164

Zhang C, Seow VY, Chen X, Too HP (2018) Multidimensional heuristic process for high-yield production of astaxanthin and fragrance molecules in *Escherichia coli*. Nat Commun 9(1):1858. doi:10.1038/s41467-018-04211-x

485 Zhang C, Zou R, Chen X, et al. (2015) Experimental design-aided systematic pathway
486 optimization of glucose uptake and deoxyxylulose phosphate pathway for improved
487 amorphadiene production. Appl Microbiol Biotechnol 99(9):3825-37. doi:10.1007/s00253-
488 015-6463-y

Tables

Table 1. Carotenoid information.

NO.	Compound	Chemical structures	RT (min)	Chemical Formula	Monoisotopic Mass (m/z)
1	β-carotene	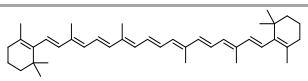	8.84	$C_{40}H_{56}$	536.438
2	lycopene	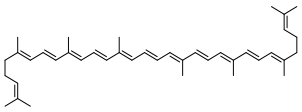	7.37	$C_{40}H_{56}$	536.438
3	echinenone	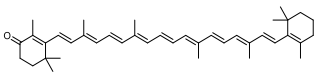	5.07	$C_{40}H_{54}O$	550.417
4	β-cryptoxanthin	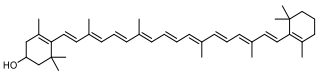	4.53	$C_{40}H_{56}O$	552.433
5	canthaxanthin	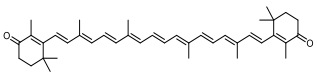	3.38	$C_{40}H_{52}O_2$	564.397
6	3'-hydroxyechinenone	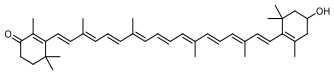	n.d.[1]	$C_{40}H_{54}O_2$	566.412
7	zeaxanthin	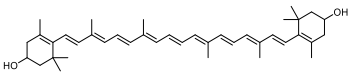	2.11	$C_{40}H_{56}O_2$	568.428
8	adonirubin	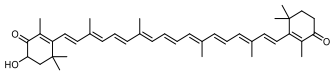	1.91	$C_{40}H_{52}O_3$	580.392
9	adonixanthin	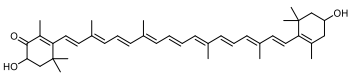	1.35	$C_{40}H_{54}O_3$	582.407
10	astaxanthin	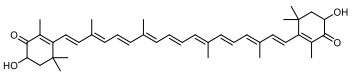	0.98	$C_{40}H_{52}O_4$	596.387
11	β-cryptoxanthin-β-D-glucoside	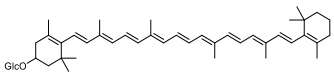	n.d.	$C_{46}H_{66}O_6$	714.486
12	3'-hydroxyechinenone-β-D-glucoside	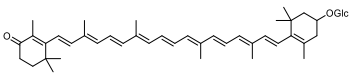	n.d.	$C_{46}H_{64}O_7$	728.465
13	zeaxanthin-β-D-glucoside	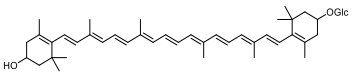	0.78	$C_{46}H_{66}O_7$	730.481
14	adonirubin-β-D-glucoside	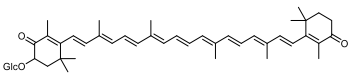	0.81	$C_{46}H_{62}O_8$	742.444

15	adonixanthin-β-D-glucoside	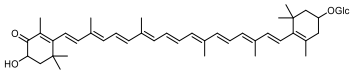	0.51	$C_{46}H_{64}O_8$	744.460
16	astaxanthin-β-D-glucoside	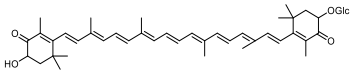	0.43	$C_{46}H_{62}O_9$	758.439
17	zeaxanthin-β-D-diglucoside	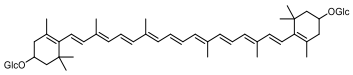	0.37	$C_{52}H_{76}O_{12}$	892.534
18	adonixanthin-β-D-diglucoside	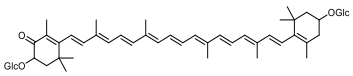	0.31	$C_{52}H_{74}O_{13}$	906.513
19	astaxanthin-β-D-diglucoside	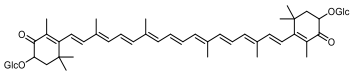	0.30	$C_{52}H_{72}O_{14}$	920.492

[1] Here, n.d. stands for not detected.

Figure legend

Fig. 1. Biosynthetic pathway of carotenoid glucosides

The biosynthetic pathway: module 1 AHT, including *atoB*, *hmgS* and *thmgR*; module 2 MPPI, including *mevk*, *pmk*, *pmd* and *idi*; module 3 EBIA, including *crtEBI* and *ispA* (Zhang et al. 2018); and module 4 YZX or YZWX, including *crtYZX* or *crtYZWX*. Dashed arrow indicates multiple enzymatic steps. The glycosylation of all carotenoids required UDP-glucose (UDP-glc), here we only used zeaxanthin glucosides as representatives. The genes expressed encode the following enzymes: *crtY*, lycopene beta-cyclase; *crtW*, β-carotene ketolase; *crtZ*, β-carotene hydroxylase; *crtX*, zeaxanthin glucosyltransferase (ZGT). Thicker and thinner arrows represent the higher and lower carbon flux, respectively; grey arrows represent that the metabolites (e.g., β-cryptoxanthin-β-D-glucoside and 3'-hydroxyechinenone-β-D-glucoside) were not detected in our strains.

Fig. 2. Production of zeaxanthin glucosides

(A) LC/MS chromatograms of zeaxanthin strains with and without the expression of *crtX*. (B) Mass spectra of zeaxanthin and its glucosides. (C) The water solutions of zeaxanthin and zeaxanthin glucosides.

Fig. 3. Tuning the translation of zeaxanthin glucosyltransferase

(A) Carotenoid contents of zeaxanthin glucoside strains. (B) OD_{600} of different strains. Error bars, mean ± s.d., n = 3. (C) Different RBSs used for *crtX* and their relative strengths. (D) Correlation between the glycosylation efficiency of zeaxanthin and the RBS strength of *crtX*. The glycosylation efficiency is defined as the percentage of zeaxanthin diglucoside yield to the total yield of zeaxanthin and its two glucosides.

Fig. 4. The effects of carbon sources on the production of zeaxanthin glucosides

(A) Carotenoid contents and OD_{600} of strain X1 by comparison of different carbon sources: 10 g/L glucose, 10g/L glycerol and their mixture, 5 g/L glucose + 5 g/L glycerol (glc+gly). (B) Carotenoid contents and OD_{600} of strains X1 and "+crtY" by optimizing the concentrations of glucose and introduction of additional copies of *crtY*. Error bars, mean ± s.d., n = 2.

Fig. 5. Structural similarity between membrane and carotenoid diglucosides and its biological benefits.

(A) Comparison between zeaxanthin and zeaxanthin glucosides strains. (B) Carotenoid distribution between cytosol and membrane. (C) Structural similarity between phospholipid bilayers and zeaxanthin diglucoside and their dimensions.

Fig. 6. Production of astaxanthin glucosides and other carotenoids

(A) The content sums of glycosylated and unglycosylated carotenoids in different strains. (B) Carotenoid contents produced in different strains. Blue: 0.03 mM IPTG; orange: 0.1 mM IPTG. 'Ast' strain is the parental astaxanthin strain without expressing *crtX*. 'GA01' is the control strain with the highest RBS strength of *crtZ*. (C) Mass spectra of astaxanthin and its glucosides.

Figures
Fig. 1

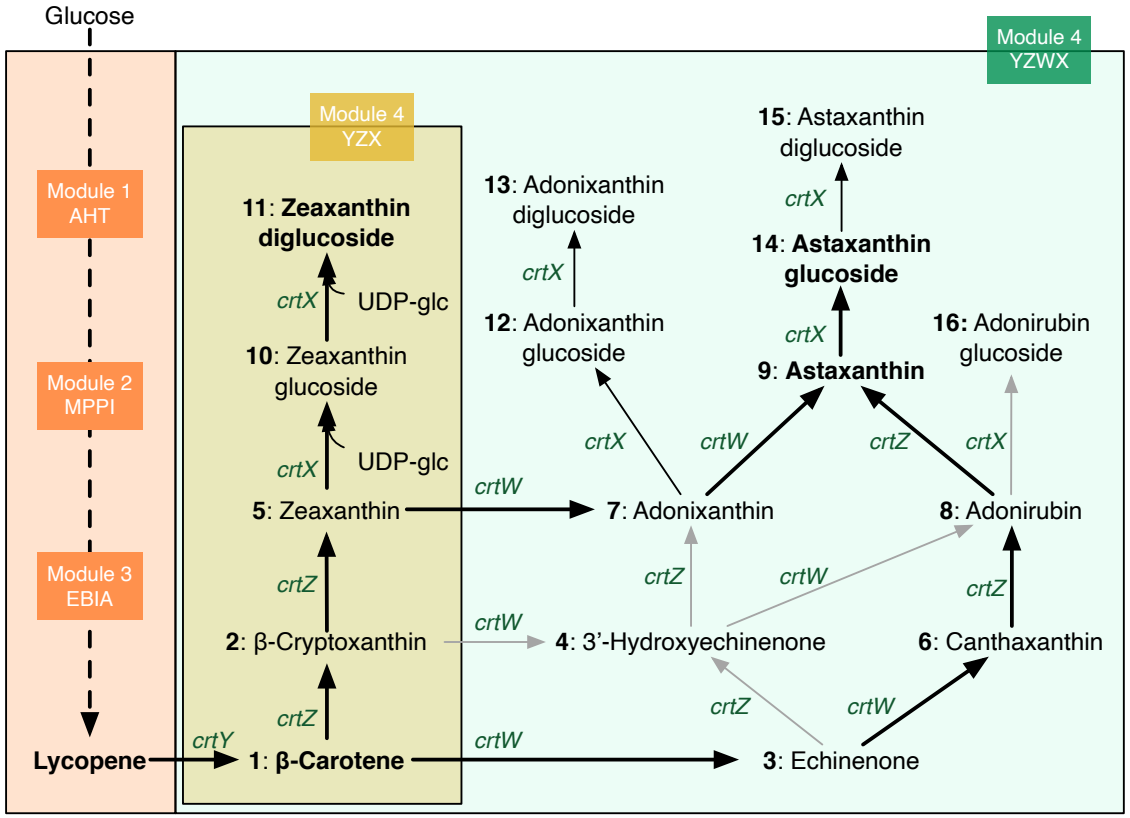

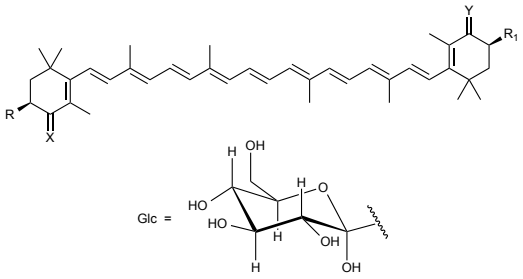

1, X=H_2, Y=H_2, R=H_2, R_1=H_2
2, X=H_2, Y=H_2, R=OH, R_1= H_2
3, X=O, Y=H_2, R= H_2, R_1= H_2
4, X=O, Y=H_2, R= H_2, R_1=OH
5, X=H_2, Y=H_2, R=OH, R_1=OH
6, X=O, Y=O, R=H_2, R_1=H_2
7, X=H_2, Y=O, R=OH, R_1=OH
8, X=O, Y=O, R=OH, R_1=H_2
9, X=O, Y=O, R=OH, R_1=OH
10, X=H_2, Y=H_2, R=OGlc, R_1=OH
11, X=H_2, Y=H_2, R=OGlc, R_1=OGlc
12, X=H_2, Y=O, R=OGlc, R_1=OH
13, X=H_2, Y=O, R=OGlc, R_1=OGlc
14, X=O, Y=O, R=OGlc, R_1=OH
15, X=O, Y=O, R=OGlc, R_1=OGlc
16, X=O, Y=O, R=OGlc, R_1=H_2

Fig. 2

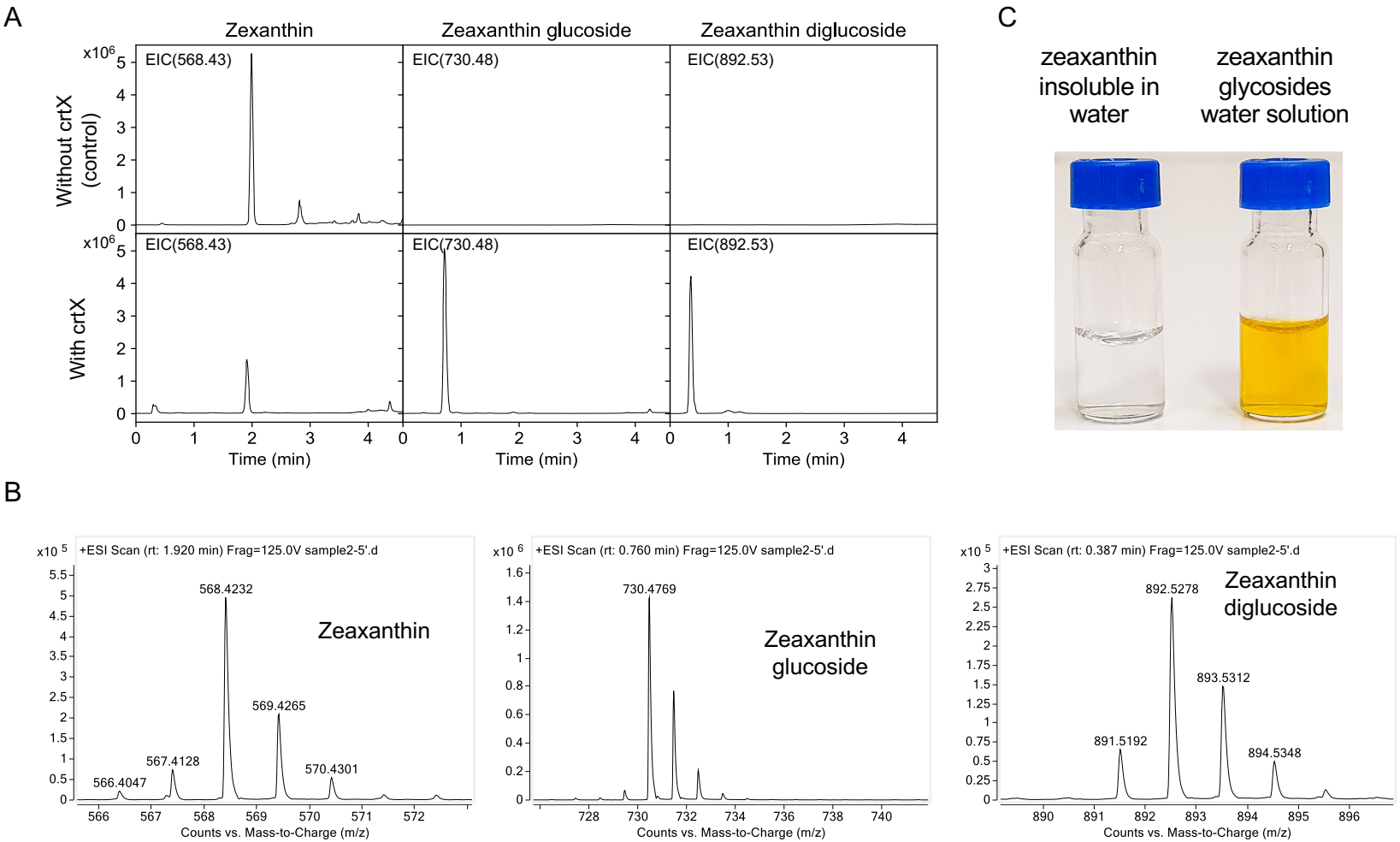
A
Zexanthin
Zeaxanthin glucoside
Zeaxanthin diglucoside
EIC(568.43)
EIC(730.48)
EIC(892.53)
Without crtX (control)
With crtX
x10^6
Time (min)
C
zeaxanthin insoluble in water
zeaxanthin glycosides water solution
B
+ESI Scan (rt: 1.920 min) Frag=125.0V sample2-5'.d
568.4232
Zeaxanthin
569.4265
567.4128
570.4301
566.4047
Counts vs. Mass-to-Charge (m/z)
+ESI Scan (rt: 0.760 min) Frag=125.0V sample2-5'.d
730.4769
Zeaxanthin glucoside
+ESI Scan (rt: 0.387 min) Frag=125.0V sample2-5'.d
892.5278
Zeaxanthin diglucoside
893.5312
891.5192
894.5348

Fig. 3

A

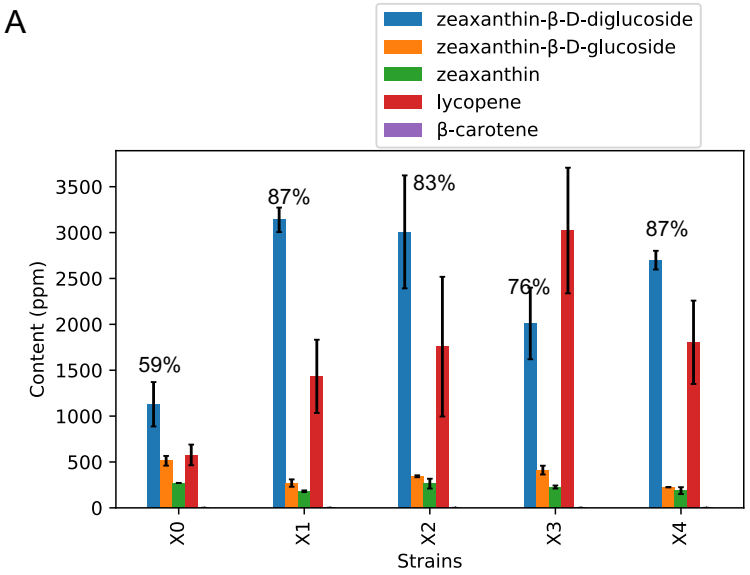

B

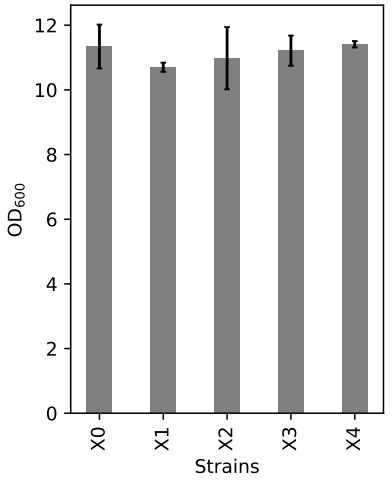

C

ID	crtX RBS sequence	Relative RBS strength
X0	acccaattcactaagcaggtcttac	0.12
X1	acccaattcactaagGaggtcttac	1.00
X2	acccaattcactaagGaggActtac	0.31
X3	acccaattcactaagGagCTcttac	0.16
X4	acccaattcactaagGagTTcttac	0.34

D

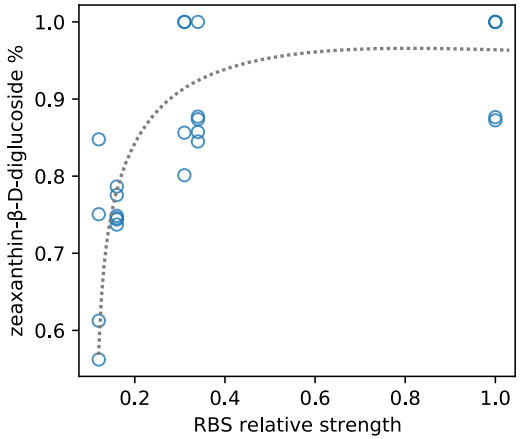

Fig. 4

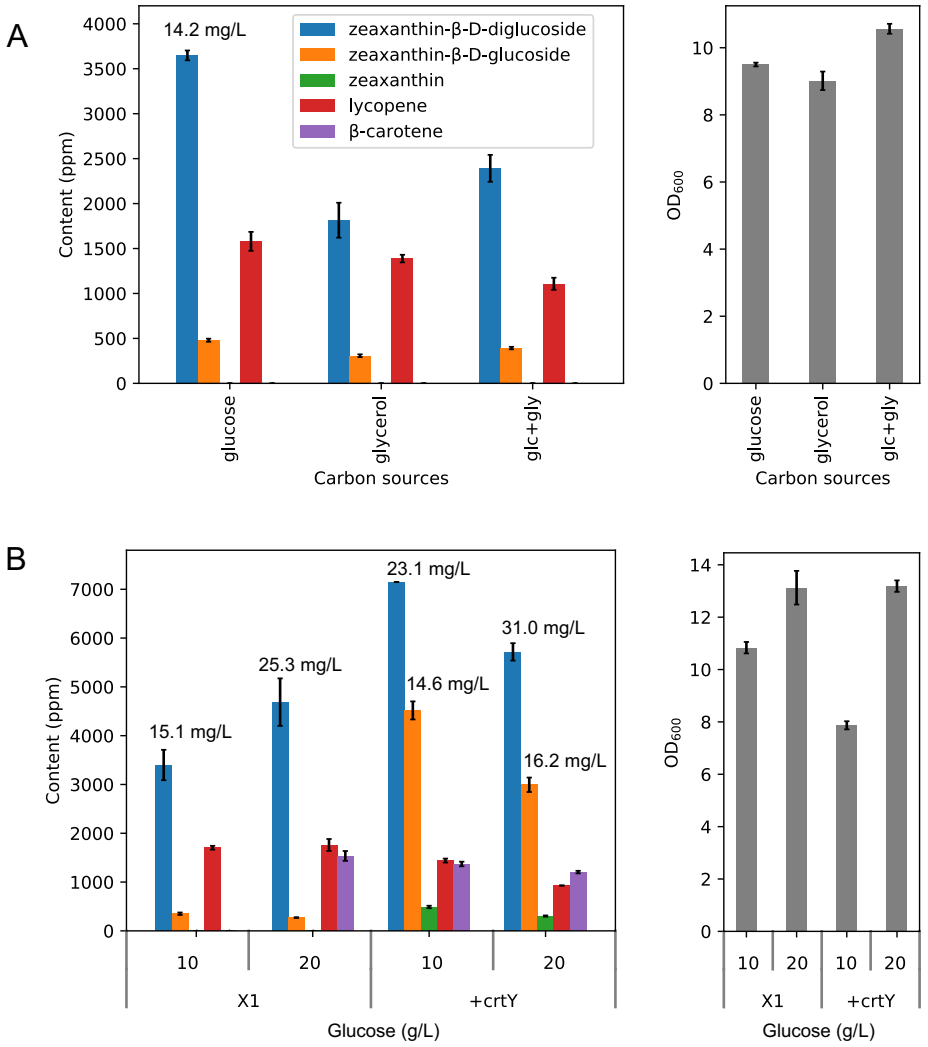
A
14.2 mg/L
zeaxanthin-β-D-diglucoside
zeaxanthin-β-D-glucoside
zeaxanthin
lycopene
β-carotene
Content (ppm)
glucose
glycerol
glc+gly
Carbon sources
OD600
B
15.1 mg/L
25.3 mg/L
23.1 mg/L
14.6 mg/L
31.0 mg/L
16.2 mg/L
X1
+crtY
Glucose (g/L)

Fig. 5

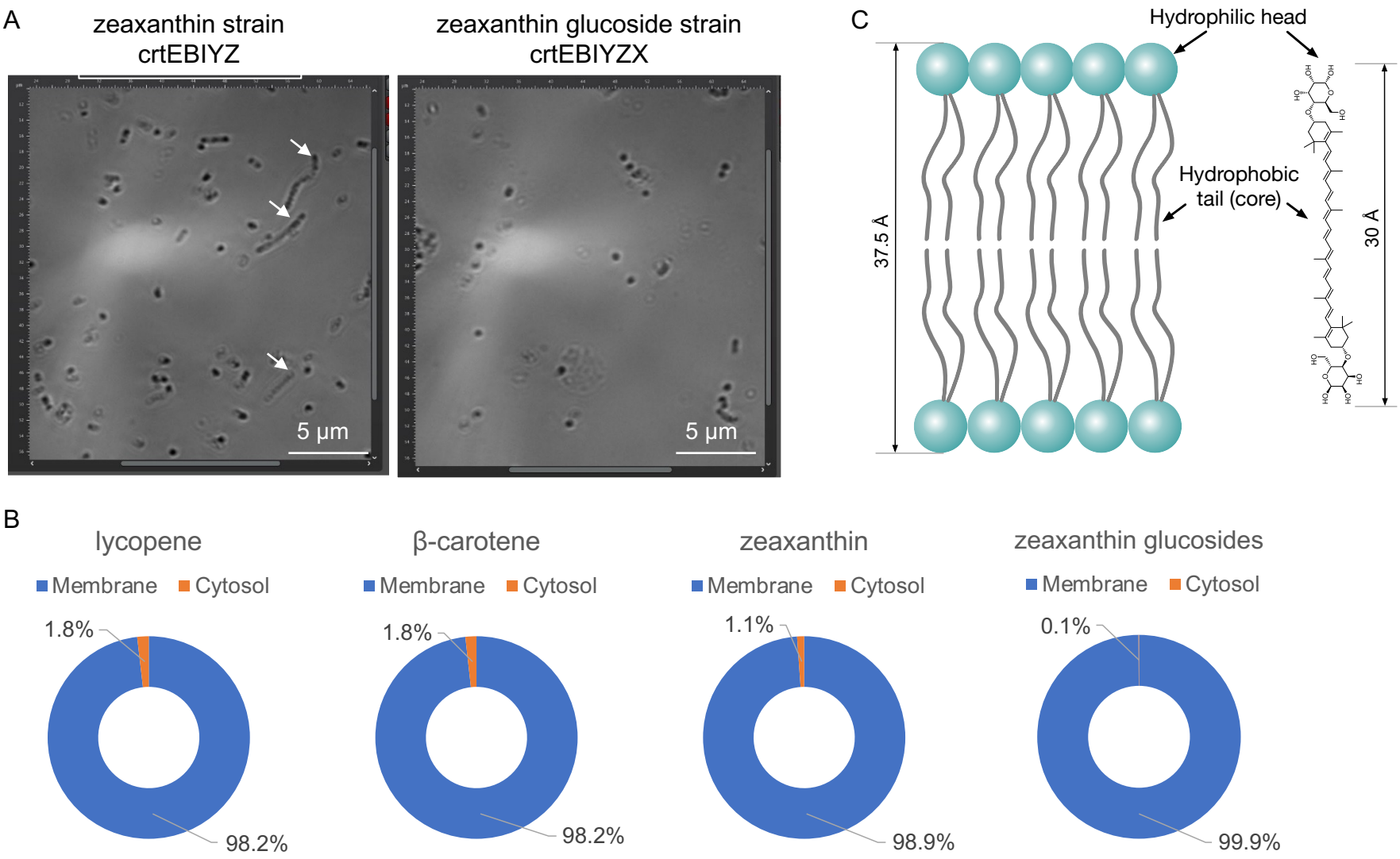
A
zeaxanthin strain
crtEBIYZ
zeaxanthin glucoside strain
crtEBIYZX
5 µm
5 µm
C
Hydrophilic head
Hydrophobic
tail (core)
37.5 Å
30 Å
B
lycopene
Membrane
Cytosol
1.8%
98.2%
β-carotene
Membrane
Cytosol
1.8%
98.2%
zeaxanthin
Membrane
Cytosol
1.1%
98.9%
zeaxanthin glucosides
Membrane
Cytosol
0.1%
99.9%

Fig. 6

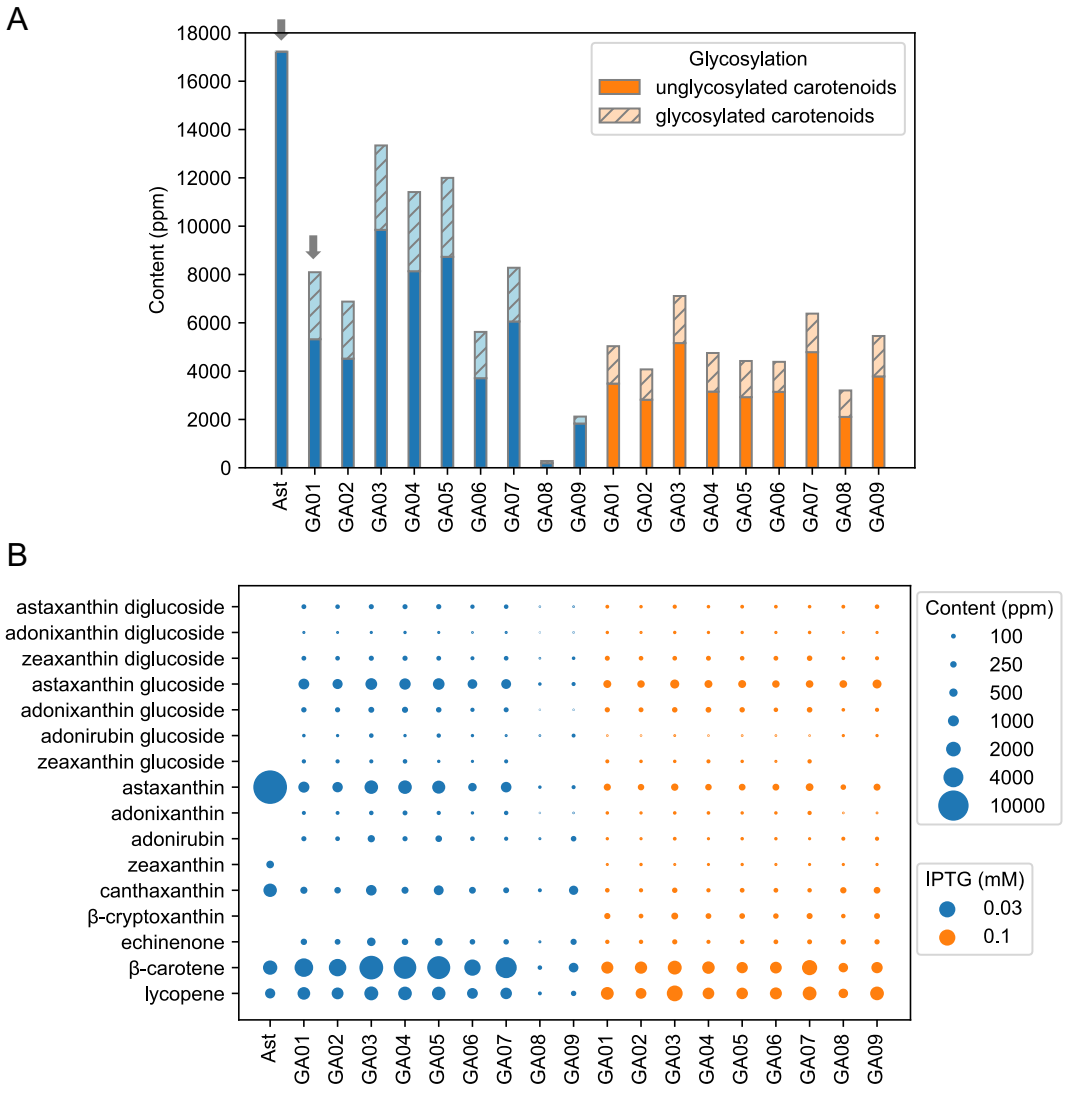
A
Content (ppm)
Glycosylation
unglycosylated carotenoids
glycosylated carotenoids
Ast
GA01
GA02
GA03
GA04
GA05
GA06
GA07
GA08
GA09
B
astaxanthin diglucoside
adonixanthin diglucoside
zeaxanthin diglucoside
astaxanthin glucoside
adonixanthin glucoside
adonirubin glucoside
zeaxanthin glucoside
astaxanthin
adonixanthin
adonirubin
zeaxanthin
canthaxanthin
β-cryptoxanthin
echinenone
β-carotene
lycopene
Content (ppm)
IPTG (mM)
0.03
0.1

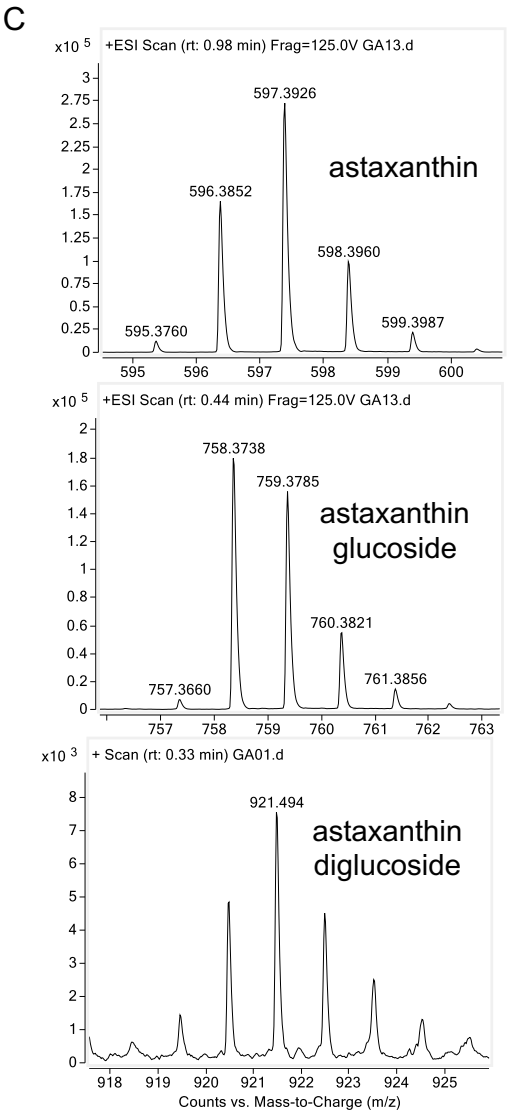
C
+ESI Scan (rt: 0.98 min) Frag=125.0V GA13.d
597.3926
596.3852
598.3960
595.3760
599.3987
astaxanthin
+ESI Scan (rt: 0.44 min) Frag=125.0V GA13.d
758.3738
759.3785
760.3821
757.3660
761.3856
astaxanthin glucoside
+ Scan (rt: 0.33 min) GA01.d
921.494
astaxanthin diglucoside
Counts vs. Mass-to-Charge (m/z)

Figures

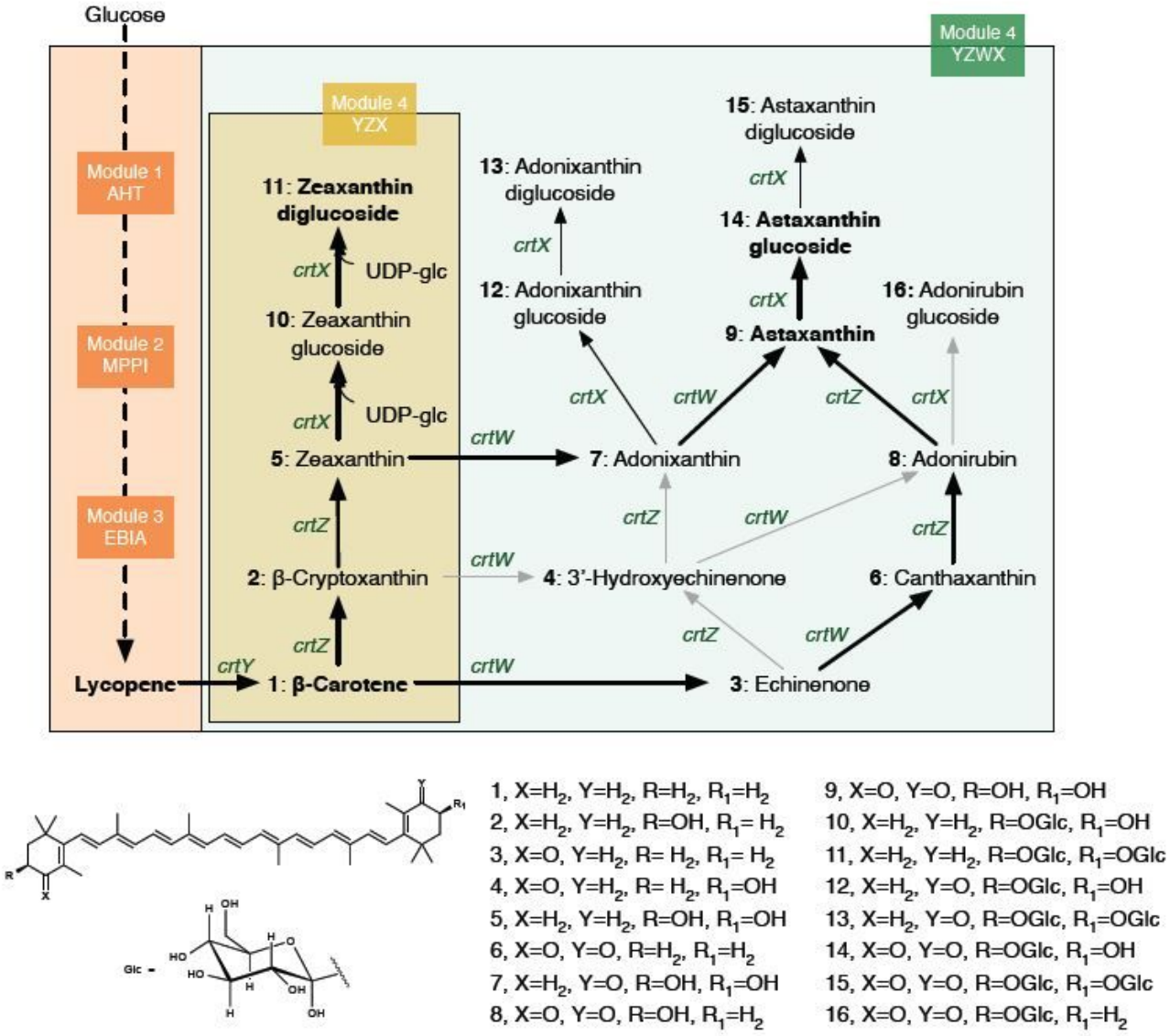

Figure 1

Biosynthetic pathway of carotenoid glucosides The biosynthetic pathway: module 1 AHT, including atoB, hmgS and thmgR; module 2 MPPI, including mevk, pmk, pmd and idi; module 3 EBIA, including crtEBI and ispA (Zhang et al. 2018); and module 4 YZX or YZWX, including crtYZX or crtYZWX. Dashed arrow indicates multiple enzymatic steps. The glycosylation of all carotenoids required UDP glucose (UDP-glc), here we only used zeaxanthin glucosides as representatives. The genes expressed encode the following enzymes: crtY, lycopene beta-cyclase; crtW, β-carotene ketolase; crtZ, β-carotene hydroxylase; crtX, zeaxanthin glucosyltransferase (ZGT). Thicker and thinner arrows represent the higher and lower carbon flux, respectively; grey arrows represent that the metabolites (e.g., β-cryptoxanthin-β-D-glucoside and 3'-hydroxyechinenone-β-D-glucoside) were not detected in our strains.

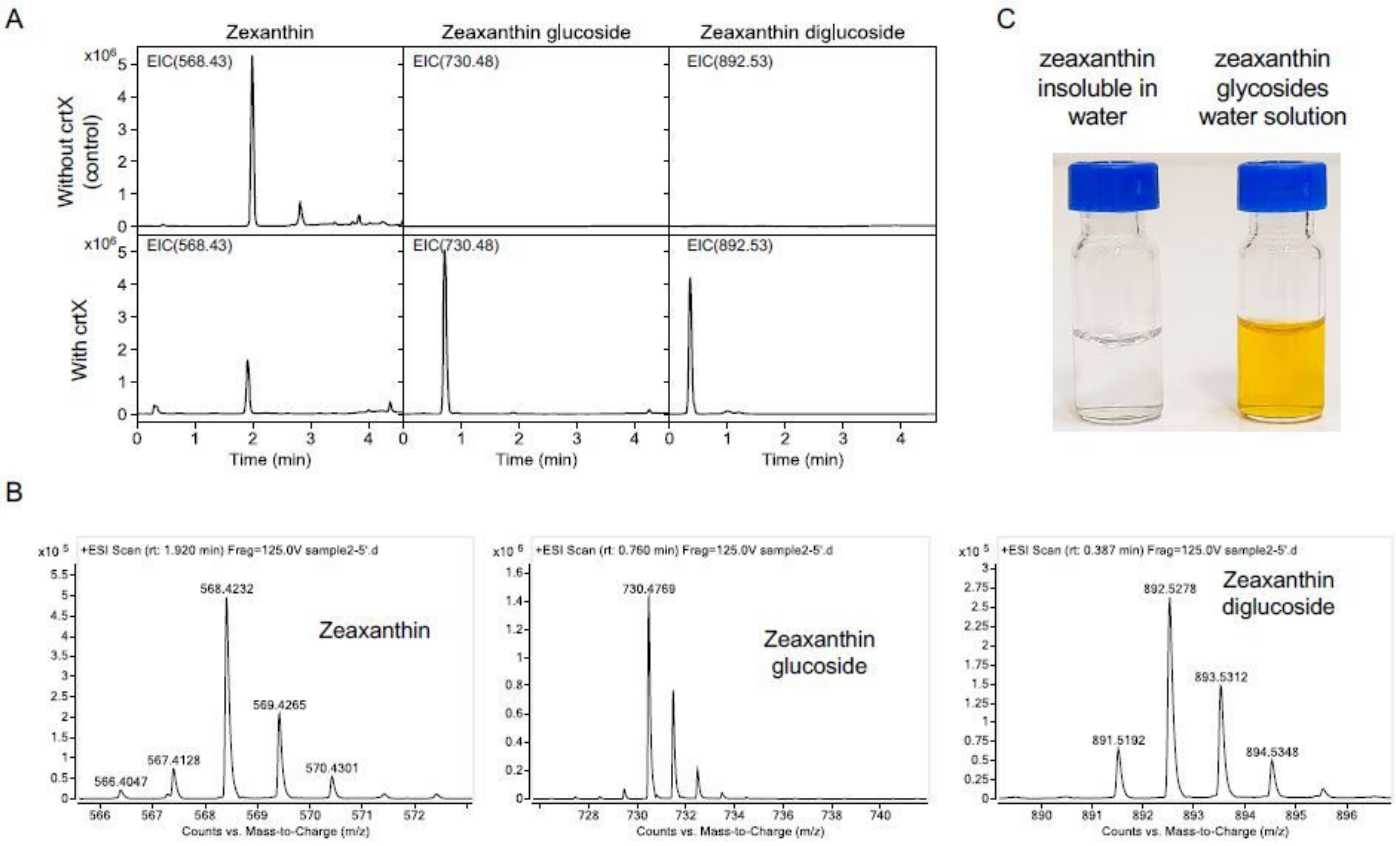

Figure 2

Production of zeaxanthin glucosides (A) LC/MS chromatograms of zeaxanthin strains with and without the expression of crtX. (B) Mass spectra of zeaxanthin and its glucosides. (C) The water solutions of zeaxanthin and zeaxanthin glucosides.

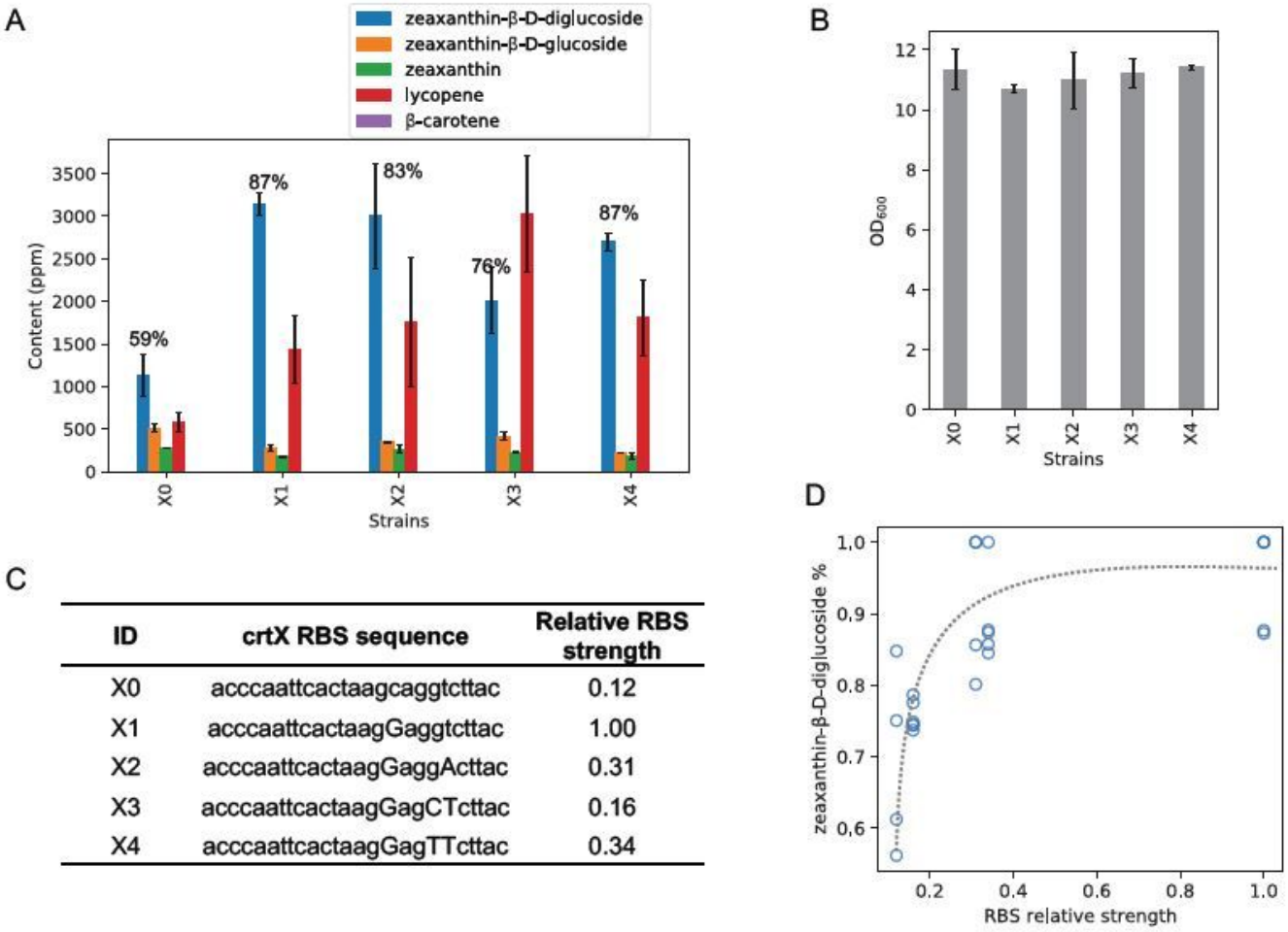

C

ID	crtX RBS sequence	Relative RBS strength
X0	acccaattcactaagcaggtcttac	0.12
X1	acccaattcactaagGaggtcttac	1.00
X2	acccaattcactaagGaggActtac	0.31
X3	acccaattcactaagGagCTcttac	0.16
X4	acccaattcactaagGagTTcttac	0.34

Figure 3

(A) Carotenoid contents of zeaxanthin glucoside strains. (B) OD600 of different strains. Error bars, mean ± s.d., n = 3. (C) Different RBSs used for crtX and their relative strengths. (D) Correlation between the glycosylation efficiency of zeaxanthin and the RBS strength of crtX. The glycosylation efficiency is defined as the percentage of zeaxanthin diglucoside yield to the total yield of zeaxanthin and its two glucosides.

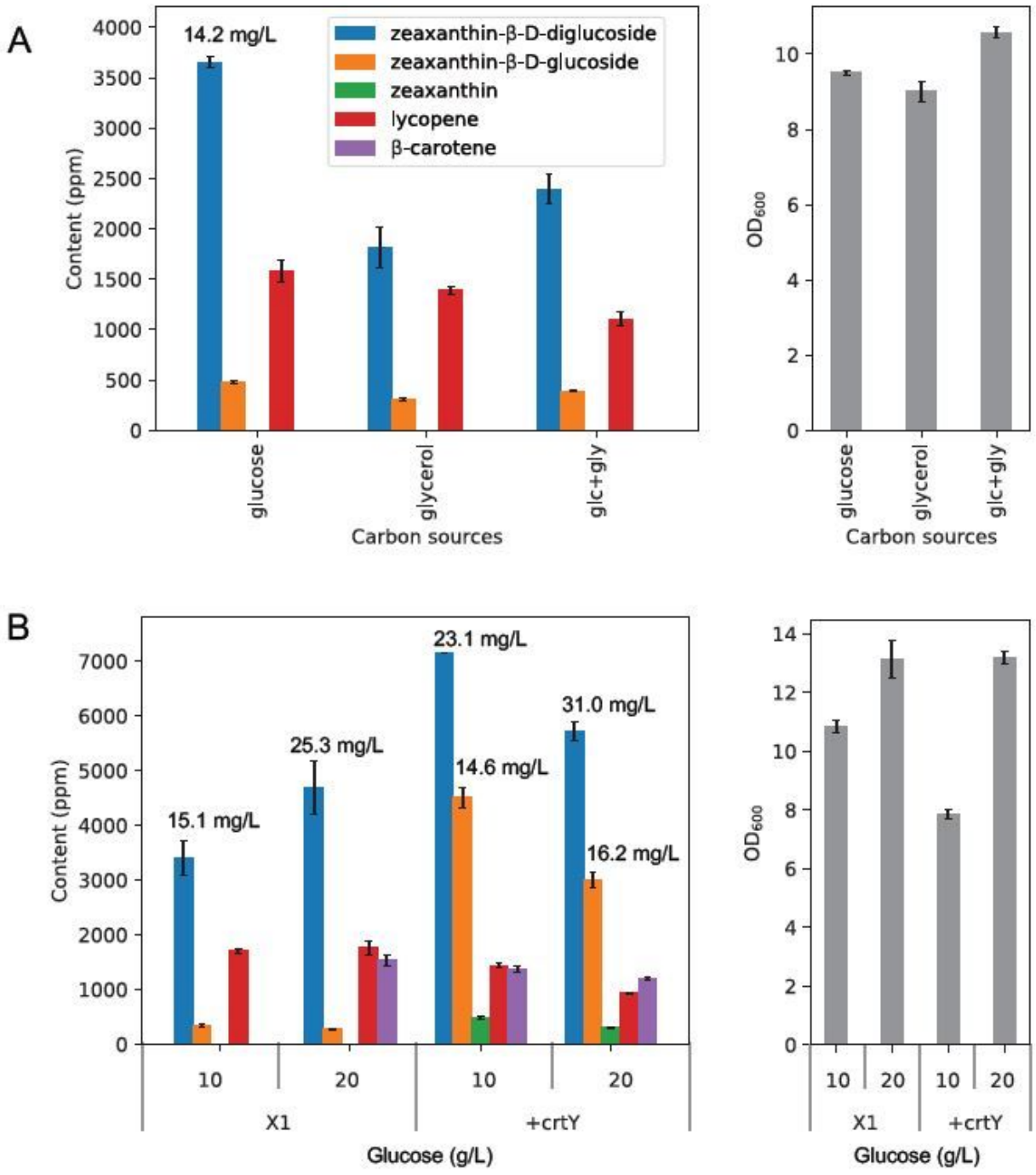

Figure 4

The effects of carbon sources on the 515 production of zeaxanthin glucosides (A) Carotenoid contents and OD600 of strain X1 by comparison of different carbon sources: 10 g/L glucose, 10g/L glycerol and their mixture, 5 g/L glucose + 5 g/L glycerol (glc+gly). (B) Carotenoid contents and OD600 of strains X1 and "+crtY" by optimizing the concentrations of glucose and introduction of additional copies of crtY. Error bars, mean ± s.d., n = 2.

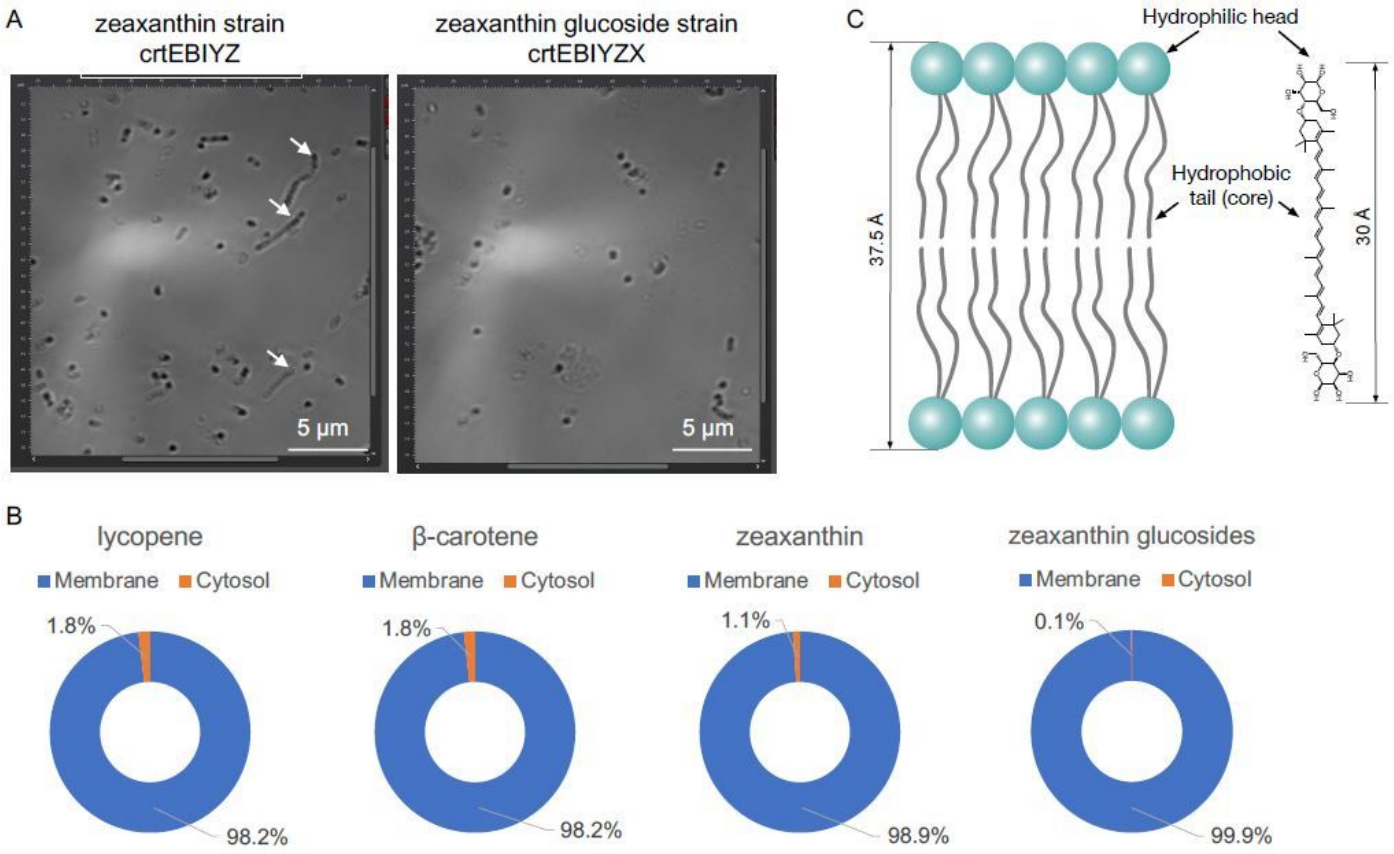

Figure 5

Structural similarity between membrane and carotenoid diglucosides and its biological benefits. (A) Comparison between zeaxanthin and zeaxanthin glucosides strains. (B) Carotenoid distribution between cytosol and membrane. (C) Structural similarity between phospholipid bilayers and zeaxanthin diglucoside and their dimensions.

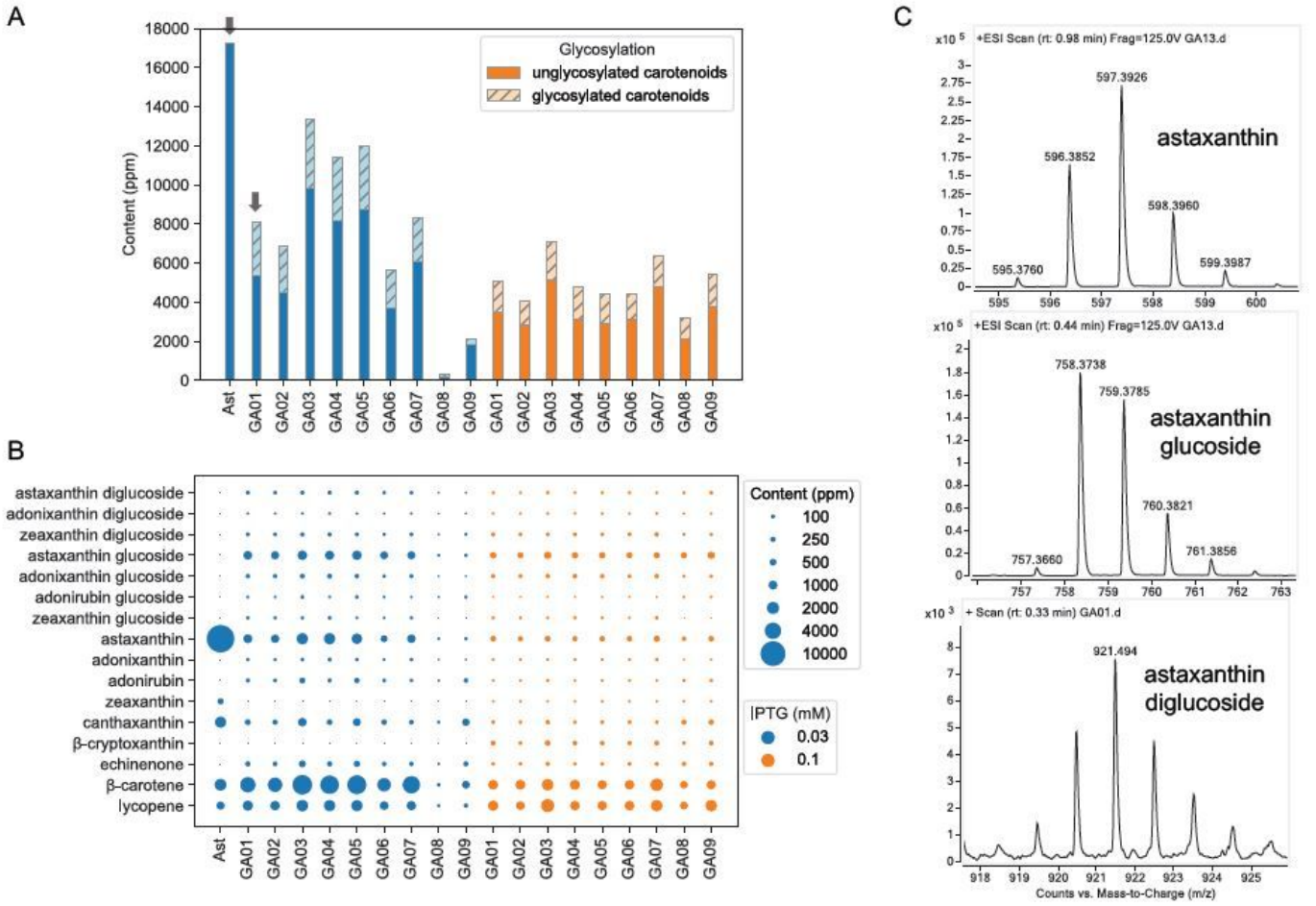

Figure 6

Production of astaxanthin glucosides and other carotenoids (A) The content sums of glycosylated and unglycosylated carotenoids in different strains. (B) Carotenoid contents produced in different strains. Blue: 0.03 mM IPTG; orange: 0.1 mM IPTG. ‘Ast’ strain is the parental astaxanthin strain without expressing crtX. ‘GA01’ is the control strain with the highest RBS strength of crtZ. (C) Mass spectra of astaxanthin and its glucosides.

Supplementary Files

This is a list of supplementary files associated with this preprint. Click to download.

- Glycosilatedcarotenoidsmanuscriptsupplementaryv5.pdf
- Graphicalabstract.jpg